# Nonreciprocal Willis Coupling in Zero-Index Moving Media

Li Quan, Dimitrios L. Sounas, and Andrea Alù

Phys. Rev. Lett. **123**, 064301 — Published 9 August 2019

DOI: 10.1103/PhysRevLett.123.064301

# Non-Reciprocal Willis Coupling in Moving Metamaterials

Li Quan[1], Dimitrios L. Sounas[1,2], and Andrea Alù[1,3,4,5,*]

[1]*Department of Electrical and Computer Engineering, The University of Texas at Austin, Austin, TX 78712, USA*

[2]*Department of Electrical and Computer Engineering, Wayne State University, Detroit, MI 48202, USA*

[3]*Photonics Initiative, Advanced Science Research Center, City University of New York, New York, NY 10031, USA*

[4]*Physics Program, Graduate Center, City University of New York, New York, NY 10016, USA*

[5]*Department of Electrical Engineering, City College of The City University of New York, NY 10031, USA*

[*]Corresponding author: aalu@gc.cuny.edu

**Mechanical motion can break the symmetry in which sound travels in a medium, but significant non-reciprocity is typically achieved only for large motion speeds. Here we combine moving media with zero-index acoustic propagation, yielding extreme non-reciprocity and induced bianisotropy for modest applied speeds. The metamaterial is formed by an array of waveguides loaded by Helmholtz resonators, and it exhibits opposite signs of the refractive index sustained by asymmetric Willis coupling for propagation in opposite directions. We use this response to induce non-reciprocal positive-to-negative sound refraction, and propose a non-reciprocal metamaterial lens focusing only with excitation from one side based on asymmetric Willis coupling.**

Reciprocity in wave propagation requires that the response of a source remains the same when source and observation points are interchanged. Breaking this symmetry allows designing devices that exhibit different transmission for opposite propagation directions, which is important for protection of sensitive equipment from external interference and for full-duplex communications. For electromagnetic waves, several approaches have been proposed to break reciprocity, including biasing with external magnetic fields [1]-[2] transistors [3]-[4], angular momentum [5]-[6], spatiotemporal modulation [7]-[8], and non-linearities [9]-[10]. In acoustics, non-reciprocal devices have been mainly realized based on nonlinear mechanisms [11]-[13]. While it is well established that sound traveling parallel or anti-parallel to a moving medium is transmitted non-reciprocally [14], strong effects are typically achieved only when the velocity of the medium is large, or in highly resonant devices [15]-[16]. Based on this principle, momentum bias applied through moving media was recently used to realize linear acoustic non-reciprocal devices [17]-[18]. In the following, we explore moving metamaterials operated around their zero-index operation, showing how in this scenario mechanical motion opens highly unusual scenarios for sound propagation. We unveil the underlying physical mechanism in presence of asymmetric Willis coupling, and use this feature to design a non-reciprocal lens which can realize focusing only from one side.

A moving medium exhibits different wave-vectors $k_+$ and $k_-$ for opposite propagation directions, which is a signature of nonreciprocity. As such, the nonreciprocal parameter

$$\eta = \left|\mathrm{Re}\left(k_+\right) + \mathrm{Re}\left(k_-\right)\right| \Big/ \left|\mathrm{Re}\left(k_+\right) - \mathrm{Re}\left(k_-\right)\right| \tag{1}$$

measures the degree of asymmetry in wave propagation for opposite directions. In absence of motion, $k_+$ and $k_-$ are necessarily the same in magnitude and with opposite signs, hence $\eta = 0$, while $\eta$ is nonzero when reciprocity is broken. In a moving medium, in absence of frequency dispersion we can write [19],[20]

$$k_{\pm} = \pm k_R + k_{NR}, \text{ with } k_R = k_0 / \left(1 - M^2\right),\ k_{NR} = -Mk_0 / \left(1 - M^2\right), \qquad (2)$$

where $k_R, k_{NR}$ are the reciprocal and non-reciprocal portions of the wavenumber, respectively, $M = U_0 / c_0$ is the Mach number, defined as the ratio of flow speed $U_0$ to the background sound speed $c_0$, and $k_0 = \omega / c_0$ is the wavenumber in free space. Replacing these quantities in (1) yields $\eta = \left| k_{NR} / k_R \right| = \left| M \right|$, implying that non-negligible non-reciprocity can be expected only for large, often impractical Mach numbers.

In order to break this trade-off and achieve large non-reciprocity with small flow speed, we explore the regime for which $k_R = 0$, i.e., zero-index propagation, so that the non-reciprocal portion of the wave-number $k_{NR}$ dominates. In electromagnetics, epsilon-near-zero (ENZ) metamaterials [21]-[22] provide a reciprocal zero index of refraction, which has been shown to lead to extreme wave propagation properties [23]-[24]. Acoustic waves in a zero-index media may therefore provide a platform to boost nonreciprocal phenomena when modest medium speeds are considered. Density-near-zero metamaterials [25]-[26], the analogue of ENZ materials for sound, have been realized in the past using waveguides loaded by membranes. However, this approach is not suitable for our purpose of realizing non-reciprocal wave transmission with the help of background flow, because conventional membranes would block the flow. We consider

therefore extreme non-reciprocal responses by imparting air flow to waveguides loaded by a Helmholtz resonator array, inducing a near-zero refractive index at rest ($k_R \approx 0$) [27], while $k_{NR} \neq 0$. In such a metamaterial, we expect that even a small mechanical motion yields a negative phase velocity (and refractive index) for propagation parallel to the fluid motion, and a positive one for propagation anti-parallel to it, hence $\eta = |k_{NR} / k_R| \to \infty$ $|M|$. In the following, we verify this response for plane-wave incidence, observing opposite refraction angles for excitation from opposite sides.

The geometry under analysis is shown in Fig. 1, and it consists of an array of parallel waveguides loaded with Helmholtz resonators. The green color indicates the region with air flow, and the geometrical parameters are provided in the caption. In order to impart air flow in each waveguide, a pipe is connected to both sides and loaded with a fan, (not shown in the figure), inducing a continuous air flow, as indicated by the arrows. To ensure that the incident acoustic wave only travels through the waveguide, we load two Helmholtz resonators at each pipe opening (not shown), designed to filter out the excitation frequencies. The structure is supplied with two matching layers at both sides (yellow color) in order to eliminate impedance mismatch, they do not support zero-index propagation, hence their width is compact. The lower inset of Fig. 1 shows the calculated Mach number along each waveguide, zero outside the moving segment, and which linearly increases to an approximately constant value of 0.1 (corresponding to a velocity of 34.3 m/s) inside the waveguide through a finite transition layer. The small fluctuations of Mach number inside the waveguide are due to the Helmholtz resonators [28]. All the details of the geometry under analysis are provided in Fig. 1. The focus of this paper is to show how moderate constant flow can induce extreme non-reciprocal wave propagation

and asymmetric Willis coupling. To keep simplicity but without losing generality, the background flow simulation has been performed with COMSOL Multiphysics, 2D Poisson's equation module [28]. The module solves $\nabla \cdot \mathbf{U}_0 = f$, where $f$ and $\mathbf{U}_0$ correspond to the source term and background flow speed. Source terms are placed at both sides of each waveguide to model the inlet and outlet connections to the pipe in the *z*-direction.

Consider now the excitation of this geometry with obliquely-incident plane waves from opposite sides, as shown in Fig. 2. The simulation is performed by COMSOL Multiphysics with Aeroacoustics Module in 2D [28] and the operation frequency is 11537 Hz. The actual background flow obtained from the simulations using the Poisson's equation Module is implemented into the Aeroacoustics Module to take into account the realistic medium flow in the waveguide. In our simulations, we use the continuity boundary conditions for acoustic pressure and particle velocity at the interface between the region with no motion and the matching layer, due to the material mismatch at these interfaces. At the interface between the region with no motion and the transition layer inside the waveguides, as well as at the one between the transition layer and the main body of the waveguide, we instead apply continuity boundary conditions for acoustic pressure and air mass flow [29]. Figure 2a presents the acoustic pressure field distribution for excitation from the left side. Due to momentum conservation, the tangential component of the wave-vector and transverse phase velocity is conserved, while the normal component changes direction across the interface, resulting in negative refraction. Quite interestingly, the situation is opposite for excitation from the right side: Figure 2(b) presents the acoustic fields for an incident wave coming from the right side at the same

incident angle. In this case, the direction of the normal component of the wave-vector does not flip as the wave enters the metamaterial, indicating positive refraction. This drastically different refraction response from opposite sides for modest values of $M$ is a signature of extreme nonreciprocity, arising from the slowly moving medium combined with the near-zero-index response in the metamaterial. Although the negative/positive phase index of the material is non-reciprocal, the energy velocity always flows away from the source, as expected from causality [30].

A better understanding of the phenomenon can be gained by extracting the effective constitutive parameters of the metamaterial. The mass conservation equation and momentum equation in each waveguide with air flow are derived in detail in [31], and take the general form

$$\partial u/\partial x = i\omega\left(E_{eff}^{-1}p + \xi_{eff}u\right) \quad (3)$$

$$\partial p/\partial x = i\omega\left(\rho_{eff}u + \varsigma_{eff}p\right), \quad (4)$$

where $E_{eff}^{-1} = \left(E_0^{-1} - F^{-1}\right)/\left(1-M^2\right)$ is the effective bulk modulus, $\rho_{eff} = \rho_0/\left(1-M^2\right)$ is the effective density, $E_0 = \rho_0 c_0^2$ is the bulk modulus in air, $\xi_{eff} = -M\,c_0^{-1}/\left(1-M^2\right)$ and $\varsigma_{eff} = M\left(\rho_0 c_0 F^{-1} - c_0^{-1}\right)/\left(1-M^2\right)$ are odd bianisotropy cross coupling coefficients arising from non-reciprocity, $F = S_w d M_a\left(\omega^2 - \omega_0^2\right)$ is a factor that depends on the geometry of the structure, and $\omega_0, M_a$ are the Helmholtz resonator resonance angular frequency and acoustical mass, respectively. The dispersion of the effective parameters in Eqs. (3)-(4) versus frequency for the metamaterial geometry is shown in [31]. We stress that this effective medium model applies over a broad range of frequencies, not limited to

the zero-index operation of the material, and it breaks down only when the wavelength in the material becomes comparable to the loading period.

The material flow introduces strong asymmetry in sound propagation, inducing what is known as *bianisotropy*, a response that is highly anisotropic in nature, as it holds only for propagation along *x*, and at the same time couples together pressure and velocity through the Willis coupling terms $\xi_{eff}$ and $\varsigma_{eff}$ [32]-[33]. The introduction of bianisotropy provides us an extra degree of freedom to control the sound propagation properties, especially relevant in the zero-index propagation regime. For a stationary waveguide loaded with Helmholtz resonators [34], which corresponds to our scenario in the limit of $M = 0$, only the bulk modulus $E_{eff}$ is affected by the loads, yielding near-zero $E_{eff}^{-1}$, corresponding to a zero index of refraction, when $E_0^{-1} = F^{-1}$. The effective density is not affected at all by the resonators. When a modest fluid motion is considered, however, the effective density and bulk modulus are weakly modified through the factor $\left(1-M^2\right)^{-1}$, but most importantly they are coupled together through the bianisotropy coefficients $\xi_{eff}$ and $\varsigma_{eff}$. Different from conventional Willis coupling [35]-[38], these coefficients do not obey reciprocity, $\xi_{eff} \neq -\varsigma_{eff}$, and are odd with respect to $M$, i.e., they flip sign for opposite propagation directions, a clear sign of non-reciprocity. As we show in [31], around the resonance of Helmholtz Resonator $\varsigma_{eff}$ goes through a resonance and flips sign, similar to $E_{eff}$, producing extremely asymmetric Willis coupling coefficients and non-reciprocal response.

By combining Eqs. (3) and (4), we derive the dispersion relation

$$k_{\pm} = \pm \frac{\omega\sqrt{\left(\xi_{eff} - \varsigma_{eff}\right)^2 + 4\rho_{eff}E_{eff}^{-1}}}{2} + \frac{\omega\left(\xi_{eff} + \varsigma_{eff}\right)}{2}, \quad (5)$$

yielding

$$k_R = \frac{\omega\sqrt{\left(\xi_{eff} - \varsigma_{eff}\right)^2 + 4\rho_{eff}E_{eff}^{-1}}}{2} = \frac{k_0 c_0}{1 - M^2}\sqrt{M^2\left(\frac{\rho_0 c_0 F^{-1}}{2}\right)^2 + \rho_0\left(E_0^{-1} - F^{-1}\right)} \quad (6)$$

$$k_{NR} = \frac{\omega\left(\xi_{eff} + \varsigma_{eff}\right)}{2} = -k_0\frac{M}{1 - M^2}\left(1 - \frac{\rho_0 c_0^2 F^{-1}}{2}\right). \quad (7)$$

Notice the strong difference between these expressions and Eq. (2), which is consistent with Eq. (5) in the limit $F^{-1} = 0$, i.e., without Helmholtz resonators. With the help of strong sound-matter interactions enabled by the metamaterial, we are able to realize zero-index $k_R$ and at the same time, a non-negligible $k_{NR}$. At $\omega = \sqrt{\omega_0^2 + \left(1 + \sqrt{1 - M^2}\right)E_0 \Big/ \left(2S_w dM_a\right)}$, $k_R = 0$, and $\eta \to \infty$, largely enhancing the non-reciprocal response, due to asymmetric Willis coupling induced by the mechanical motion. In this regime the wavenumber reads

$$k_{\pm} = k_{NR} = -k_0\frac{M}{\left(1 + \sqrt{1 - M^2}\right)\sqrt{1 - M^2}}, \quad (8)$$

enabling opposite refractive index for opposite directions of propagation. Interestingly, the wavenumber in the metamaterial has the same real value for both propagation directions, i.e., no matter whether the incident wave is coming from left or right, the wavevector has the same direction and value, anti-parallel to the fluid motion, consistent with our numerical simulations in Fig. 2. We stress that for $k_R = 0$ the effective bulk modulus is negative, $E_{eff}^{-1} = -\left(\xi_{eff} - \varsigma_{eff}\right)^2 \Big/ \left(4\rho_{eff}\right)$, and the effective density positive,

$\rho_{eff} = \rho_0 / \left(1 - M^2\right)$, yet the acoustic wave travels in the metamaterial without decay because of the strong Willis coupling response.

Figure 3 shows the wavenumber dispersion in Eq. (5). In absence of air flow ($M = 0$), the dispersion has a cut-off at the zero-index condition $E_0^{-1} = F^{-1}$, and it is strictly even with respect to $k$, as expected from reciprocity. When a moderate air-flow is turned on ($M = 0.1$), the dispersion diagram is asymmetric, as expected for a nonreciprocal medium, and the cutoff frequency shifts down to $\omega = \sqrt{\omega_0^2 + \left(1 + \sqrt{1 - M^2}\right) E_0 \Big/ \left(2 S_w d M_a\right)}$. Around this frequency, waves propagating in opposite directions have a nonzero (negative) wavenumber, independent of the propagation direction, and the non-reciprocity coefficient $\eta$ is very large. While in this Letter zero-index is achieved at the waveguide cut-off, similar operation may be envisioned in other zero-index metamaterials, such as around Dirac points [39]-[41].

The non-reciprocal Willis coupling induced through mechanical motion in Eq. (5) can also be used to create a lens that focuses a source placed at one side, but with diverging properties when a source is placed on the other side. The focusing operation is achieved by imparting a phase shift across the structure that transforms a diverging circular wavefront to a converging one [31], which is achieved tailoring the air flow velocity across different channels to accumulate the required phase at each aperture. Our design is shown in Fig. 4(a), where we plot the relation between Mach number, maintained below 0.09 in each channel, and the channel number $n$, with $n = 0$ being the channel on the same axis as the source ($y = 0$). The air flow in each channel is symmetric with respect to the $y$-axis (i.e., for channels $N$ and $-N$ the air flow is the same), so we only

show the imparted Mach number for positive $n$. Figure 4(b) shows the calculated acoustic pressure distribution when the sound source is located on the left of the lens: after travelling through the planar metamaterial, a focused image is constructed at the right side of the lens. Figure 4(c) presents instead the pressure distribution when the sound source is located at the right side of the lens: here we only get a divergent wave, demonstrating strong nonreciprocity with modest required flow velocities. The operation frequency here has been raised to 16 kHz to enhance the transmission for each different channel with different background flow. Operating away from the resonance frequency ensures that detuning each channel to achieve the desired phase pattern at the lens output does not affect the transmission amplitude through each channel, and that the response in time is very fast, as discussed in [31].

By adjusting the air flow in each channel, we can achieve different functionalities. In Figs. 4d-f we show a design that converts a point source to a plane wave only when the source is located on the right side of the metamaterial. Again, the relation between channel number and Mach number is presented in Fig. 4(d), while Figs. 4e-f show the acoustic pressure profile when the source is located at the two sides of the structure, highlighting again the strongly non-reciprocal response.

In conclusion, we have presented here a Willis metamaterial operating near the zero-index operation, yielding extreme non-reciprocal responses with modest air flow. These unusual acoustic properties are the result of a non-reciprocal bianisotropic response dominating the effective properties of the metamaterial, as the reciprocal response tends to zero. For this reason, even modest air flows can provide highly unusual responses, including opposite (positive-to-negative) refractive index for opposite propagation

directions, and non-reciprocal lenses. Within the proposed Willis metamaterial, the air flow can be modulated in real-time to reconfigure the properties of the metamaterial, making it an exciting platform to control sound beyond the conventional limitations of natural materials. We envision a plethora of applications of these concepts, from ultrasound imaging to sonar technology, with possible extensions to the realm of phononics and surface acoustic waves. We also expect exciting opportunities stemming from the introduction of nonlinearities in this zero-index metamaterial platform [42], which may combine large non-reciprocity and Willis coupling, small direct linear responses and enhanced nonlinear interactions with sound.

**Reference**


[1] Z. Wang, Y. Chong, J. D. Joannopoulos, and M. Soljacic, Observation of unidirectional backscattering-immune topological electromagnetic states. *Nature* **461**, 772-775 (2009).

[2] F. D. M. Haldane, and S. Raghu, Possible realization of directional optical waveguides in photonic crystals with broken time-reversal symmetry. *Phys. Rev. Lett.* **100**, 013904 (2008).

[3] T. Kodera, D. L. Sounas, and C. Caloz, Artificial Faraday rotation using a ring metamaterial structure without static magnetic field. *Appl. Phys. Lett.* **99**, 031114 (2011)

[4] B. I. Popa, and S. A. Cummer, Nonreciprocal active metamaterials, *Phys. Rev. B* **85**, 205101 (2012).

[5] D. L. Sounas, C. Caloz, and A. Alù, Giant non-reciprocity at the subwavelength

scale using angular momentum-biased metamaterials, *Nat. Commun.* **4**, 2407 (2013).

[6] N. Estep, D. Sounas, J. Soric, and A. Alù, Magnetic-free non-reciprocity based on parametrically modulated coupled-resonator loops, *Nat. Phys.* **10**, 923 (2014).

[7] H. Lira, Z. Yu, S. Fan, and M. Lipson, Electrically driven nonreciprocity induced by interband photonic transition on a silicon chip. *Phys. Rev. Lett.* **109**, 033901 (2012).

[8] D. Wang, H. Zhou, M. Guo, J. Zhang, J. Evers, and S. Zhu, Optical diode made from a moving photonic crystal, *Phys. Rev. Lett.* **110**, 093901 (2013).

[9] S. Lepri, and G. Casati, Asymmetric wave propagation in nonlinear system. *Phys. Rev. Lett.* **106**, 164101 (2011).

[10] M. Soljacic, C. Luo, J. D. Joannopoulos, and S. Fan, Nonlinear photonic crystal microdevices for optical integration. *Opt. Lett.* **28**, 637 (2003).

[11] B. Liang, B. Yuan, J. C. Cheng, Acoustic diode: rectification of acoustic energy flux in one-dimensional system. *Phys. Rev. Lett.* **103**, 104301 (2009).

[12] B. Liang, X. S. Guo, J. Tu, D. Zhang, J. C. Cheng, An acoustic rectifier, *Nat. Mater.* **9**, 989 (2010).

[13] N. Boechler, G. Theocharis, C. Daraio, Bifurcation-based acoustic switching and rectification. *Nat. Matter.* **10**, 665 (2011).

[14] L. M. Brekhovskikh, I. P. Lysanov, *Fundamentals of Ocean Acoustics* (Springer, Berlin, 2003).

[15] Y. Xiao, B. R. Mace, J. Wen, and X. Wen, Formation and coupling of band gaps in a locally resonant elastic system comprising a string with attached

resonators, *Phys. Lett. A* **375**, 1485-1491 (2011).

[16] Y.-F. Wang, V. Laude, and Y.-S. Wang, Coupling of evanescent and propagating guided modes in locally resonant phononic crystals, *J. Phys. D: Appl. Phys.* **47**, 475502 (2014).

[17] R. Fleury, D. L. Sounas, C. F. Sieck, M. R. Haberman, and A. Alu, Sound isolation and giant linear nonreciprocity in a compact acoustic circulator, *Science* **343**, 516 (2014).

[18] R. Fleury, D. L. Sounas, and A. Alu, Subwavelength ultrasonic circulator based on spatio-temporal modulation, *Phys. Rev. B* **91**, 174306 (2015).

[19] P. M. Morse and K. U. Ingard, Theoretical Acoustics, Princeton University Press, (1987).

[20] A. Lakhtakia, V. K. Varadan, and V. V. Varadan, Green's functions for propagation of sound in a simply moving fluid. *J. Acoust. Soc. A* **85**, 1852 (1989).

[21] A. Alu, M. G. Silveirinha, A. Salandrino and N. Engheta, Epsilon-near-zero metamaterials and electromagnetic sources: tailoring the radiation phase pattern, *Phys. Rev. B* **75**, 155410 (2007).

[22] B. Edwards, A. Alu, M. E. Young, M. Silverinha, and N. Engheta, Experimental verification of epsilon-near-zero metamaterial coupling and energy squeezing using a microwave waveguide, *Phys. Rev. Lett.* **100**, 033903 (2008).

[23] I. Liberal, and N. Engheta, Near-zero refractive index photonics, *Nat. Photon.* **11**, 149-158 (2017).

[24] I. Liberal, A. M. Mahmoud, Y. Li, B. Edwards, and N. Engheta, Photonic doping of epsilon-near-zero media, *Science* **355**, 1058-1062 (2017).

[25] R. Fleury and A. Alu, Extraordinary sound transmission through density-near-zero ultranarrow channels, *Phys. Rev. Lett*. **111,** 055501 (2013).

[26] Y. Gu, Y. Cheng, X. Liu, Acoustic planar hyperlens based on anisotropic density-near-zero metamaterials, *Appl. Phys. Lett.* **107,** 133503 (2015).

[27] L. Quan, X. Zhong, X. Liu, X. Gong and P. A. Johnson, Effective impedance boundary optimization and its contribution to dipole radiation and radiation pattern control, *Nat. Commun.* **5,** 3188 (2014).

[28] The numerical simulations here and in the following are performed using COMSOL Multiphysics, https://www.comsol.com/

[29] G. K. Bachelor, An Introduction to Fluid Dynamics, Cambridge University Press, (2000).

[30] J. B. Pendry, Negative refraction makes a perfect lens, *Phys. Rev. Lett.* **85**, 3966 (2000).

[31] See Supplementary Material for a detailed description of the geometry, a derivation of the mass conservation and momentum equations, the dispersion relation of the effective parameters, the design details of the non-reciprocal lens and the time evolution of the non-reciprocal lens.

[32] J. A. Kong, Theorems of bianisotropic media, *Proc. IEEE* **60**, 1036-1046 (1972).

[33] G. W. Milton, M. Briane, and J. R. Willis, On cloaking for elasticity and physical equations with a transformation invariant form, *New J. Phys.* **8**, 248 (2006).

[34] N. Fang, D. Xi, J. Xu, M. Ambati, W. Srituravanich, C. Sun and X. Zhang,

Ultrasonic metamaterials with negative modulus, *Nat. Mater.* **5**, 452 (2006).

[35] J. R. Willis, Variational principles for dynamic problems for inhomogeneous elastic media, *Wave Motion* **3**, 1 (1981).

[36] A. N. Norris, A. L. Shuvalov, and A. A. Kutsenko, Analytical formulation of three-dimensional dynamic homogenization for periodic elastic system, *Proc. R. Soc. A* **468**, 1629 (2012).

[37] L. Quan, Y. Ra'di, D. L. Sounas and A. Alu, Maximum Willis coupling in acoustic scatterers, *Phys. Rev. Lett.* **120**, 254301 (2018).

[38] C. F. Sieck, A. Alu and M. R. Haberman, Origins of Willis coupling and acoustic bianisotropy in acoustic metamaterials through source-driven homogenization, *Phys. Rev. B* **96**, 104303 (2017).

[39] F. Liu, X. Huang, and C. T. Chan, Dirac cones at $\vec{k} = 0$ in acoustic crystals and zero refractive index acoustic materials, *Appl. Phys. Lett.* **100**, 071911 (2012).

[40] X. Changqing, G. Ma, Z.-G. Chen, J. Luo, J. Shi, Y. Lai and Y. Wu, Three-dimensional acoustic double-zero-index medium with a Dirac-like point, arXiv:1901.08830 (2019).

[41] Observation of acoustic Dirac-like cone and double zero refractive index, *Nat. Commun.* **8**, 14871 (2017).

[42] C. Argyropoulos, P. Y. Chen, G. D'Aguanno, N. Engheta, and A. Alu, Boosting optical nonlinearities in $\varepsilon$-near-zero plasmonic channels, *Phys. Rev. B* **85**, 045129 (2012).

**Figures**

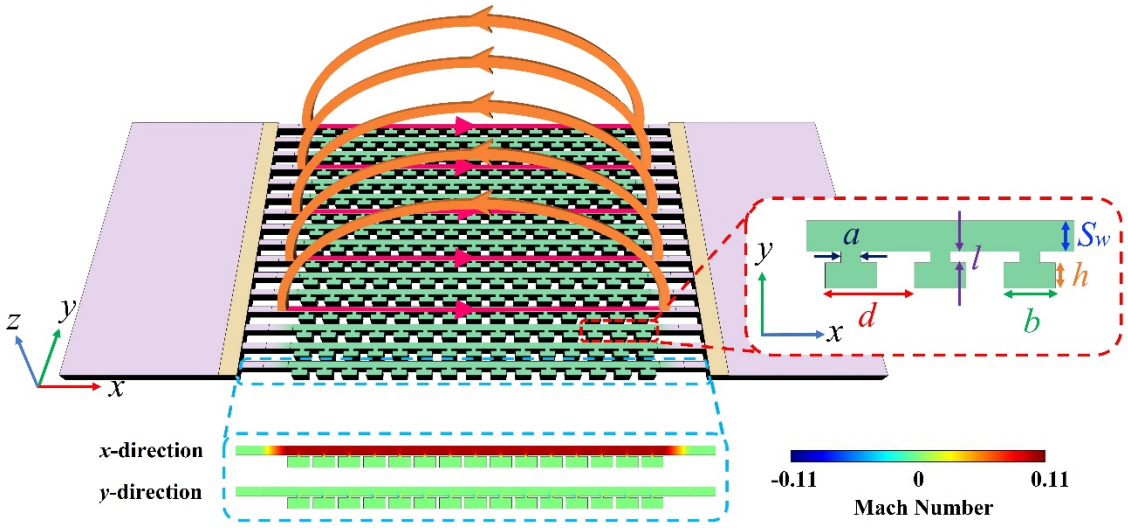


Fig. 1. Geometry of the nonreciprocal metamaterial, formed by an array of parallel waveguides loaded by Helmholtz resonators (green). A constant air flow inside the waveguides is generated by fans (red color and orange color indicate the flow inside the waveguide and the flow outside the *x*-*y* plane in the pipe, respectively). The waveguides have a width $S_w$=3 mm, a distance $d$=8 mm between neighboring resonators, which have a neck length $l$=0.5 mm, a neck width $a$=1 mm, a cavity length $b$=7 mm and a cavity width $h$=3.5 mm. Two sets indicate the Mach number distribution in the waveguide between two matching layers and the enlarged structure of our microstructures, respectively.

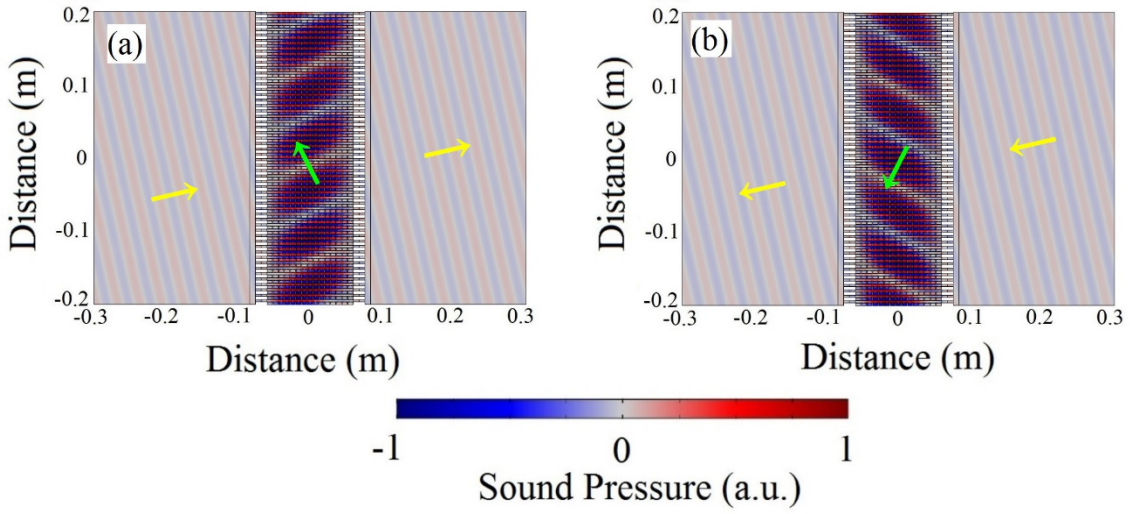


Fig. 2. (a) Acoustic pressure distribution for an incident wave coming from the left. The yellow arrows indicate the wave vector in air and the green arrow indicates the wave vector in the metamaterial. (b) Acoustic pressure distribution for an incident wave coming from the right.

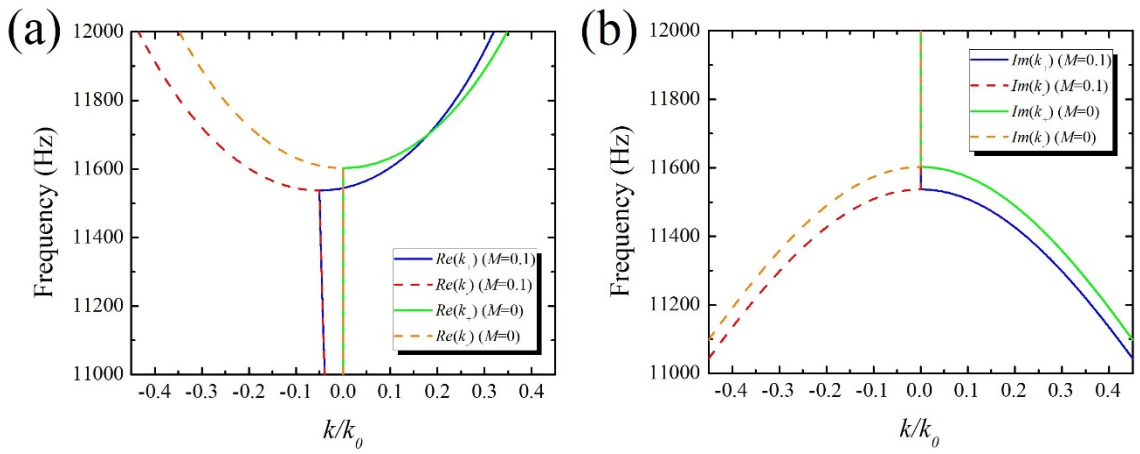


Fig. 3. Dispersion diagram for the geometry of Fig. 1 calculated from Eq. (5). (a) Real part. (b) Imaginary part.

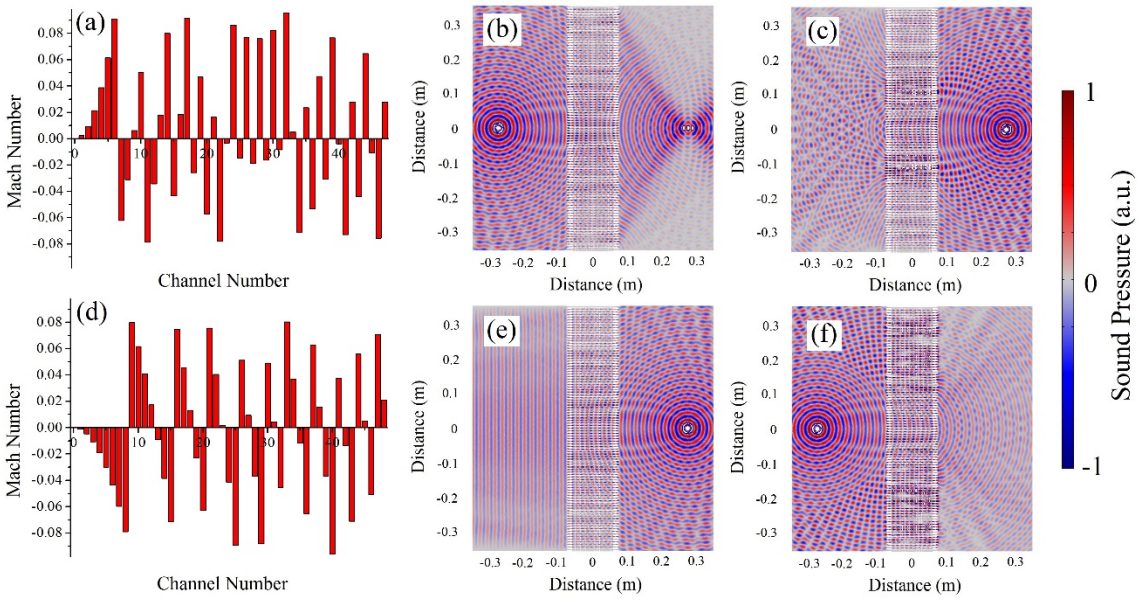


Fig. 4. (a) Modulation of the Mach number in each channel to synthesize a focusing lens. (b) Acoustic pressure distribution when the source is located on the left side of the lens. A focused image is obtained on the right. (c) Acoustic pressure distribution when the source is located on the right of the lens. (d) Modulation of the Mach number to synthesize a point-source to plane wave converter. (e) Acoustic pressure distribution when the source is located on the right. A plane wave is induced on the left side. (f) Acoustic pressure distribution when the source is located on the left side.